Performance Analysis of DC Motors With Integrated Proportional-Integral and Artificial Neural Network Control

Mukhlidi Muskhir [1], Afdal Luthfi [1], Muldi Yuhendri [1], Aswardi Aswardi [1], Aprilla Fortuna [1]

[1]*Faculty of Engineering, Universitas Negeri Padang, Padang, Indonesia*

Abstract – **Direct current (DC) motors are frequently utilized in various applications, and the motor's pace is affected by applied loads as it fluctuates. A power converter must be employed to control the velocity of the motor by varying the armature voltage. One of the options for the power converter is the one-quadrant DC chopper. In this case, the investigation will turn the one-quadrant chopper into a system by merging velocity and current control into the DC motor. The speed is regulated by controlling the armature voltage. This may be accomplished using a controlled rectifier. The contribution of the research is to test the effectiveness of Artificial Neural Network Control (ANN) and Proportional-Integral (PI) controllers to control the speed of a DC motor using a one-quadrant DC chopper. Therefore, due to technological advancements, the authors will utilize the training data of the artificial neural network of Proportional-Integral controllers in MATLAB's Simulink. Test results demonstrate the artificial neural network (ANN's) superior ability to regulate system response, showing enhancements in delay time, rise time, overshoot, and steady-state error compared to the PI controller. These findings underscore the potential of ANN as a more sophisticated choice for DC motor control, although further research is required to fine-tune its performance through rigorous training.**

Keywords – **Artificial neural networks, motor DC, proportional-integral, one quadrant DC chopper**

1. Introduction

The DC motor transforms electrical energy into mechanical energy through magnetic fields generated with direct current [1], [2], [3]. Due to their versatility, DC motors have extensive use in diverse industrial and domestic settings. They operate with direct current (DC) voltage, but a notable issue encountered is speed fluctuation induced by varying loads, resulting in inconsistent motor performance [4], [5]. DC motors have characteristics that can be controlled for speed, torque, and rotor position [6]. The DC motor control system supervises and regulates the motor's operational path. One approach to regulating the speed of a DC motor involves modifying its armature or field current [7]. This can be accomplished by varying the motor voltage through a power converter like a controlled rectifier or DC chopper.

The DC chopper serves as a voltage converter for DC, providing control over the output voltage [8]. Choppers, like AC transformers, convert voltages, but they employ rapid on-off switches to transform a DC input voltage into a variable DC output voltage. DC choppers come in various types, including one quadrant, two quadrants, and four quadrants [9]. The choice of DC chopper type relies on the specific operational requirements of the motor, particularly within the DC motor's operating quadrant.

This study employs a one-quadrant DC chopper to regulate DC motor speed by adjusting the armature current through stator voltage control. Stator voltage is modulated using pulse width modulation (PWM) to achieve the desired speed control. Apart from PWM, the PID (proportional-integral-derivative) control method is also utilized for speed regulation. However, contemporary technological advancements have led to significant changes, particularly in motor speed control systems, which now incorporate various models and methods, including artificial intelligence (AI) [10].

Artificial neural network (ANN), a form of artificial intelligence, has gained popularity for controlling DC motors [11].

ANNs are mathematical models that mimic the structure and function of nerves found in biological systems [12]. ANNs can comprehend intricate and non-linear data patterns. In DC motor control, they discern the connection between inputs (like applied voltage) and outputs (like motor speed). Utilizing this knowledge, ANNs produce an optimal control signal to attain desired objectives. Their primary strength lies in managing the complexities, uncertainties, and disruptions inherent in DC motors. Additionally, ANNs can adapt and learn from system variations, enhancing the control system's reliability and effectiveness [13].

The research employs ANN to investigate its viability as an alternative controller, utilizing test data from a PI controller, which remains a prevalent choice in the industry. It assesses multiple control parameters, including time response and disturbance handling, to compare ANN's performance with the PI controllers. Achieving parity with the PI controller's performance suggests the potential for integrating intelligent control into process systems through further advancements.

2. Literature Review

In this section, there will be a background study and literature review regarding research that has been conducted by others related to this research. The aim is to understand the theoretical foundations and concepts that underlie the control methods used. This research combines proportional-integral (PI) control technique with artificial neural network (ANN) to improve the performance of DC motors. Therefore, the following literature review will present a comprehensive explanation of artificial neural network (ANN), back-propagation artificial neural network, direct current (DC) motor, and DC chopper one quadrant, which forms the basis for the performance analysis to be conducted.

2.1. Artificial Neural Network (ANN)

An artificial neural network (ANN) is a synthetic model that mimics the learning process of the human brain, also known as a human neural network (HNN) [14]. Certain principles governing the operation of the human neural network pertain to information storage and memory [15]. Repeated transmission of a particular signal through a synapse enhances its efficacy in transmitting the signal subsequently.

This principle forms the foundation of the learning process, necessitating extensive training of the ANN before its effective utilization.

Artificial neural networks, an artificial intelligence component, operates on the principle of connections, drawing inspiration from human neural networks [16]. The operational concept involves neurons receiving multiple combined signals and being assessed against a threshold. A response is generated if the signal weights are appropriately configured. Artificial neural networks (ANNs) emulate the brain's neural networks' information processing, serving various functions in machine learning, including pattern recognition, classification, and prediction [16], [17], [18]. The ANN's mathematical model comprises interconnected nodes (neurons) that process input data and transmit outputs to subsequent layers of nodes.

In the ANN, neurons are fundamental units that receive input from other neurons or external sources, process it, and produce an output [19]. Neuronal behaviour in the ANN is typically determined by input weights and activation functions [20]. Input weights represent the strength or significance of each input (x1) to the neuron, denoted by weights (w1). Activation functions transform inputs into desired outputs, like sigmoid, hyperbolic tangent (tanh), and rectified linear unit (ReLU).
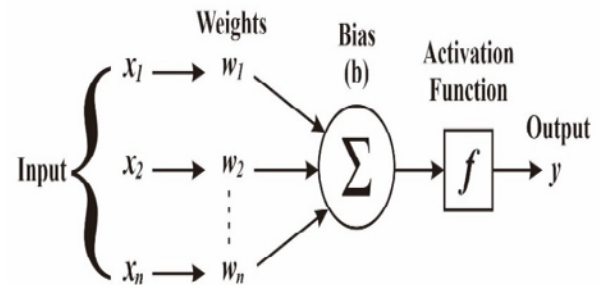

Figure 1. Mathematical model of ANN control

Figure 1 illustrates a mathematical model depicting the control system employing ANN, where the output (y) of a single neuron is represented mathematically by the following equations (1).

$$y = f\left(\Sigma i\left(wi \cdot xi\right) + b\right) \qquad (1)$$

In this context, xi represents input values, wi denotes weights, b is the bias term, and f is the activation function.

2.2. Back-Propagation Artificial Neural Network

Artificial neural network (ANN) with the back-propagation method is a type of network that involves guided training [21].

ANN comprises layers of neurons and adjusts neuron weights based on output errors in the opposite direction [22].

The initial stage involves forward propagation to calculate the output error.

Activation functions, typically involving logarithmic functions, are chosen for their continuity, differentiability, and monotonicity properties. Furthermore, the dataset's values are initially set. Training data is represented in vector format, where each input data corresponds to a specific target.

The activation function selection is contingent upon the requirements and intended outcomes. This study's chosen activation functions are tensing and linear/purely. The tansig function represents a tangent sigmoid function utilized as a transfer function [23]. This function utilizes the hyperbolic tangent sigmoid formula to transform the input value into the output. The output range of this function spans from -1 to 1. Figure 2 depicts the graphical representation of the tansig and purelin functions.
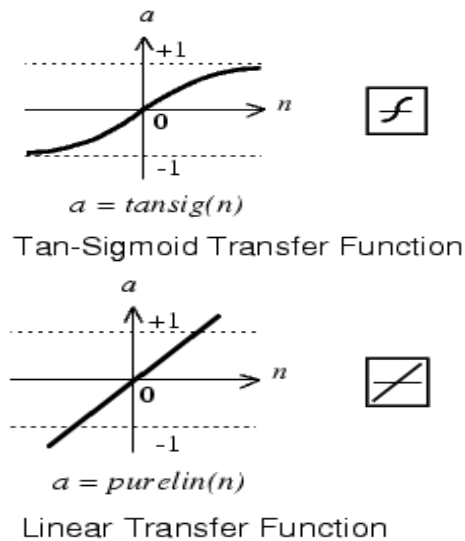

Figure 2. Activation functions of tansig and purelin

$$a = \tan sig(n) = \frac{2}{1+\exp(-2*n)} - 1 \qquad (2)$$

The linear activation function, or purelin, linearly relates the input to the output. Equation (3) represents the formula of the purelin activation function, where the parameter k denotes an arbitrary constant.

$$a = kn \qquad (3)$$

The training process of ANN through back-propagation typically comprises three phases: the forward propagation stage, the backward propagation stage, and the weight adjustment stage [24]. In the feed-forward stage, input data is propagated from the input layer to the output layer.

In the subsequent backward phase, each output unit calculates the output error, reflecting the difference between the observed and intended output, and transmits this difference backward.

The weight adjustment phase is implemented to minimize the error.

These three phases persist until a predetermined stopping condition is met.
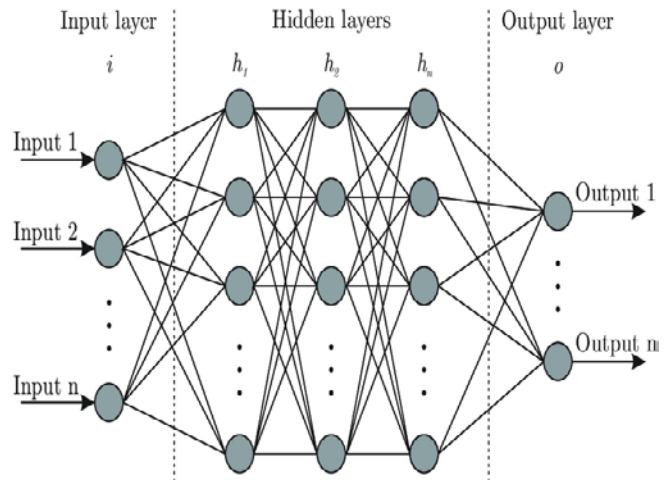

Figure 3. Architecture of the back-propagation ANN algorithm

Figure 3 depicts the back-propagation technique structure, which includes three layers: input, hidden, and output. The input layer transmits the input signal X to the hidden layer, where calculations occur based on neuron weights and biases. These calculations, governed by the activation function, determine the output values for both layers.

2.1. Motor Direct Current (DC)

The DC motor is an apparatus that transforms electrical energy, particularly in the direct current (DC) form, into mechanical energy [25]. When an electrical current traverses the coils inside a DC motor, it generates a magnetic field enveloping the armature coil in a distinct configuration. The fixed component of a DC motor, housing the field coil, is termed the stator. Conversely, the rotor, accommodating the armature coil, constitutes the motor part in motion, inducing rotation.

This research centres on a specific category of DC motors termed separately excited types. This particular DC motor requires two distinct voltage sources for operation: one for the armature coil and another for the field coil [26]. The stationary winding in a DC motor is called the stator, while the rotating winding is termed the rotor. DC motors can operate as generators; conversely, DC generators can function as DC motors when interacting with magnetic fields [27].

Figure 4 illustrates the configuration of the separately excited DC motor planned for examination in this research.
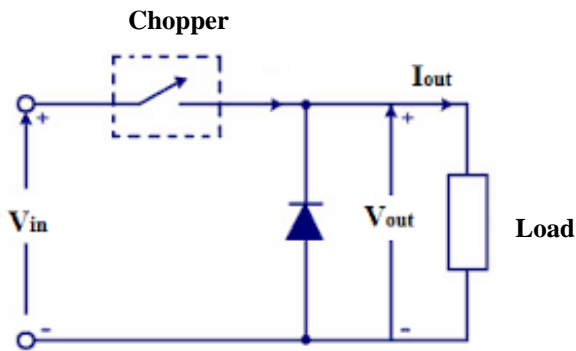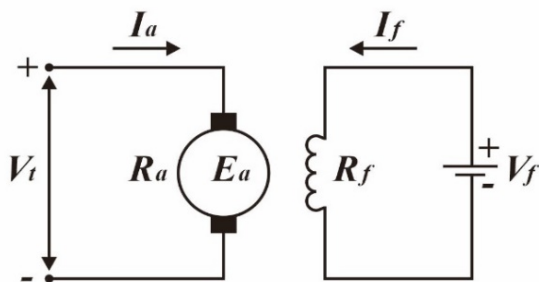
Figure 4. Schematic of separate amplifier DC motor

Figure 5. Schematic circuit of one quadrant DC Chopper motor

The equation for the separately excited DC motor is as follows.

$$Vt = Ea + IaRa \tag{4}$$

$$Vf = If + Rf \tag{5}$$

The equation represents various parameters of the separately excited DC motor, including Vt for armature terminal voltage (V), Ia for armature current (A), Ra for armature resistance (ohm), If for field current (A), Rf for field resistance (ohm), Vf for field terminal voltage (V), and Ea for electromotive force (V). The general formula for the speed of the separately excited DC motor is represented by ωm.

$$\omega m = \ Ia \tag{6}$$

Vt represents the motor's terminal voltage, Ia signifies the armature current, Ra denotes resistance, and Ta signifies the electromagnetic torque. From Equation (6), it can be deduced that adjusting the armature current or the voltage at the motor terminals facilitates the control of a DC motor's speed.

This manipulation of the armature current can be executed using a power converter by altering the modulation of the converter switch.

In this study, the utilized power converter is a one-quadrant DC chopper capable of operating the motor in the first quadrant, referred to as a forward motoring operation.

2.3. DC Chopper One Quadrant

A DC chopper is an electronic apparatus that modulates the voltage and current supplied to a DC motor by intermittently breaking the DC voltage circuit [28]. This process involves employing semiconductor devices like transistors or thyristors to manage current flow through the motor. A DC chopper serves as a DC power converter, facilitating the adjustment of its output voltage, hence commonly employed in regulating electrical devices reliant on DC voltage sources, such as DC motors. Depending on its switch configuration, a DC chopper can be categorized into three types: one-quadrant, two-quadrant, and four-quadrant [29].

This research employs a one-quadrant DC chopper operating within the first quadrant of a quadrant system. In this quadrant, the motor exclusively rotates forward using direct current and voltage, termed forward current and forward voltage [30]. The diagram depicting this one-quadrant DC chopper is presented in Figure 5.

3. Methodology

This research employs an experimental methodology to devise and formulate a DC motor speed control system. The system is constructed around a one-quadrant DC chopper featuring an ANN controller. Initial data is derived from PID control system test results and undergoes four stages: data collection, architecture selection, training, and testing. A comparative analysis of DC motor speed was conducted between the PI and ANN control systems. Data analysis involves testing the response of a second-order system and assesses four specific parameters: Delay time, which measures the time it takes for the output response to demonstrate a delay relative to the input; This time delay is computed from t = 0 until the response reaches half (50%) of its steady-state level; Rise time is the duration for the response to intersect the first steady-state axis from t = 0; Overshoot denotes the ratio between the maximum response value exceeding the steady-state value and the steady-state value itself; Steady-state error expresses the ratio between the maximum response value exceeding the steady-state value and the steady-state value [31].

The study utilizes Simulink Matlab R2020a for design and simulation.

Figure 6 illustrates the design of a DC motor speed control system employing a one-quadrant DC Chopper with an ANN controller, including components like the DC motor, DC chopper, speed control, and current control. Additionally, Figure 7 and Figure 8 depict control system designs using PI and ANN, respectively.
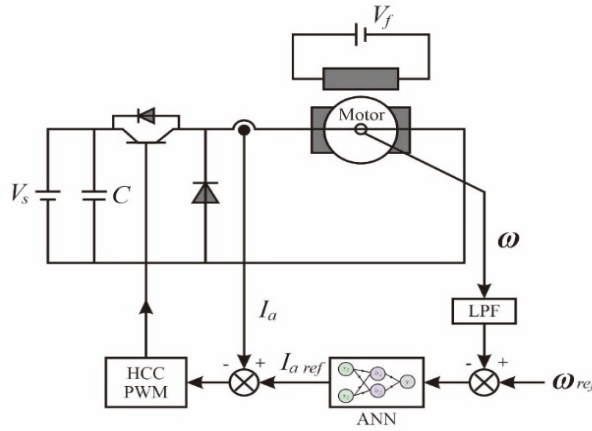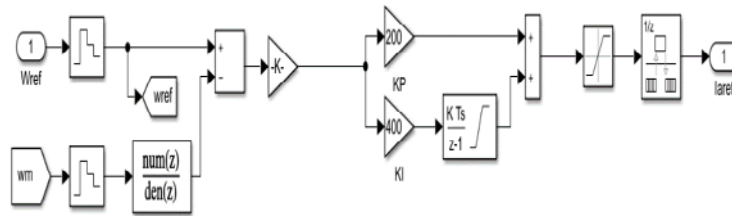

Figure 6. Schematic of separate amplifier DC motor

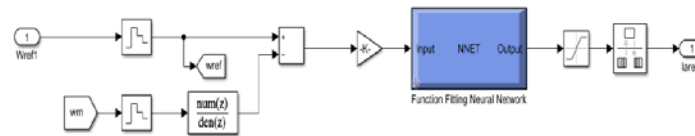*Figure 7. Design schematic of a speed control system using PI.*

Figure 8. Design schematic of a speed control system using ANN

4. Results

This section displays the pathway of the collection of input and output data, through the initiation stage of ANN architecture, subsequently the training regimen explanation and data-testing.

4.1. Collection of Input and Output Data

The procedure involves gathering input and output data from the PI controller, which will be utilized to train the artificial neural network using the back-propagation method.

The PI values employed are KP = 200 and KI = 400. Figure 9 depicts the PI controller's circuitry scheme for obtaining input and output data. This process utilizes the 'view log signal' functionality accessible in Simulink.
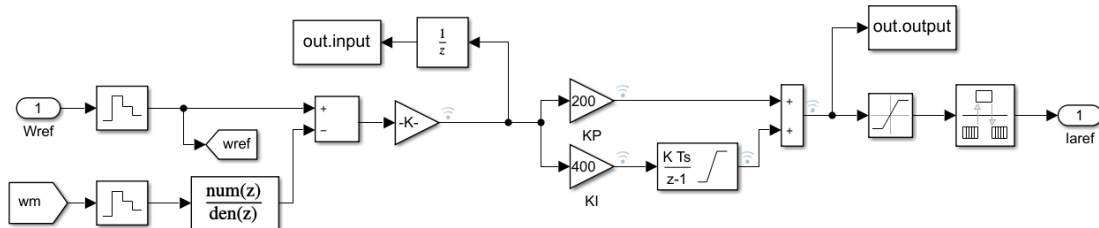

Figure 9. Schematic of the input and output data-taking circuit in the log view signal tool

During Simulink execution, the input and output data will be observable in the Matlab workspace, as depicted in Figure 10.

The acquired input and output data manifest as a matrix with dimensions of 100001x1. These datasets will facilitate the training of the artificial neural network (ANN) using the back-propagation technique.
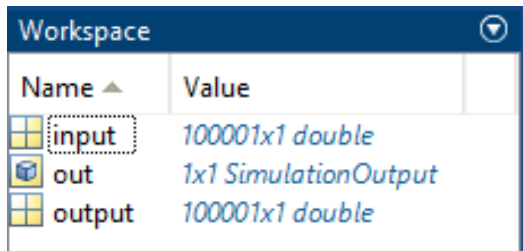

Figure 10. The results of input and output in the workspace view

4.2. Selection of Back-Propagation ANN Architecture

Upon acquiring the input and target data intended for training, the subsequent stage involves initiating the ANN training process utilizing the toolbox tool in the Matlab command window. The initial step encompasses configuring the data, commencing with data validation, and selecting the ANN architecture designated for the training regimen. Initially, the data is trained using a tool to import the input and target data from the workspace into the neural network data manager. Following data importation, the subsequent action entails configuring a training network, offering a range of options. Figure 11 illustrates the parameters for training, validation, and testing of the data scrutinized in ANN.
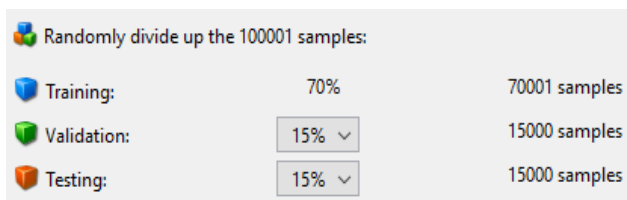

Figure 11. Validation of configuration parameters and test data

In the parameter configuration, training data will be utilized to adjust network data during the training process, adapting it based on errors encountered. Validation assesses the network's generalization capacity and ceases the training procedure when improvements in generalization halt. Conversely, testing does not influence the training process but provides an independent evaluation of network performance during and post-training.

In this instance, 70% of the data is allocated for training, yielding 70,001 samples; 15% is reserved for validation, yielding 15,000 samples, and another 15% is designated for testing, yielding 15,000 samples. This training regimen involves five layers, with the network architecture depicted in Figure 12.
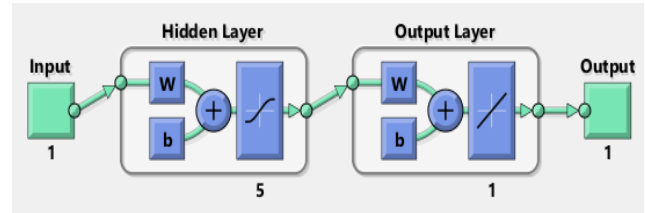

Figure 12. Architecture of ANN

4.3. Training Data for Back-Propagation ANN

The subsequent phase involves network training within the neural network data manager window after successfully establishing parameter configuration and selecting ANN architecture. The training utilizes the Levenberg-Marquardt algorithm, with the network's results depicted in Figure 13.

	Samples	MSE	R
Training:	70001	8.60278e-2	9.99463e-1
Validation:	15000	8.62876e-2	9.99451e-1
Testing:	15000	8.52094e-2	9.99433e-1

Figure 13. Results of training network on ANN

From the neural network training outcomes, there are distinct values for MSE (Mean Squared Error) and R. During training, MSE is 8.60278e-2 with an R-value of 9.99463e-1. In the validation phase, MSE is 8.62876e-2 with an R-value of 9.99451e-1. In the testing phase, MSE is 8.52094e-2 with an R-value of 9.99433e-1.
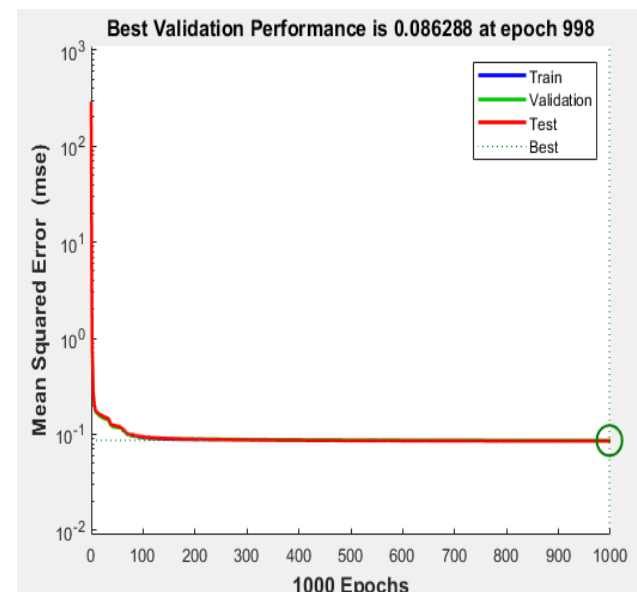

Figure 14. Results of MSE performance on ANN

Figure 14 displays the outcomes of the ANN training network, reflecting the optimal validation performance achieved during the network training process. These results demonstrate the best validation performance of 0.086288 attained at the 998th epoch out of 1000.

4.4. Testing Data for Back-Propagation ANN

Following the training of the back-propagation ANN method with the provided training dataset, the subsequent phase involves evaluating the performance of the trained back-propagation ANN against the PID controller. This comparison is conducted using the Simulink tool. To facilitate this comparison, it is imperative to ensure that the setpoints and loads employed exhibit similarities as outlined in Table 1 parameters.

Table 1. Parameter of variable speed and load on the motor

Variable	Model No. 1	Model No.2
Speed (rpm)	[300, 700, 500]	[0, 4, 7]
Load torque (N/m)	[10, 15]	[0, 3]

Table 1 presents the speed and load parameters for the motor under investigation. Regarding speed, there are three transitions: starting from 300 rpm at t = 0, rising to 700 rpm at t = 4 seconds, and then decreasing to 500 rpm at t = 7 seconds. Similarly, the torque load comprises two instances: starting at 10 Nm at t = 0 and increasing to 15 Nm at t = 3 seconds.

Figures 13 and 14 depict the outcomes of evaluating the DC motor speed control system utilizing a one-quadrant DC chopper with both PI and ANN controllers.

These results are illustrated through four graphical representations showing motor speed, load torque, armature current, and armature voltage waveforms. Figures 15 and 16 elaborate on the results of testing the DC motor speed control system employing a one-quadrant DC Chopper with PI and ANN controllers. These results are presented through four diagrams depicting waveforms of motor speed, load torque, armature current, and armature voltage.
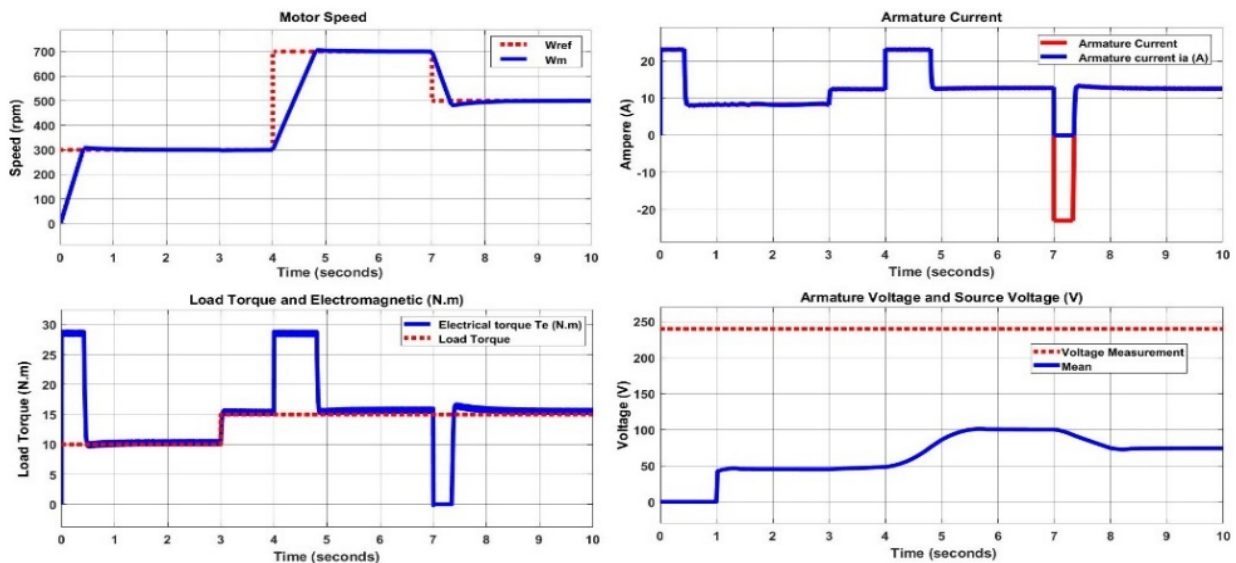

Figure 15. Results of waveforms in the control using PI

Figure 15 illustrates the performance of the PI controller in managing load and reference speed variations, albeit with some motor speed overshoot. This suggests a need to fine-tune the PI controller parameters to minimize overshoot and achieve quicker settling times while maintaining stability. The armature current and voltage graphs demonstrate the controller's efficacy in regulating motor performance. Moreover, the relationship between load and electromagnetic torque indicates the system's responsiveness to changes in load conditions.

The interplay among motor speed, armature current, load torque, electromagnetic torque, and armature and source voltages reveals a well-coordinated control system. The motor speed closely tracks the reference, indicating the controller's adeptness at achieving and sustaining the desired speed amidst setpoint changes. Fluctuations in armature current correspond to speed variations, necessitating adjustments to ensure adequate torque generation. Additionally, the electromagnetic torque adapts to load changes, ensuring the motor can manage varying loads efficiently and effectively.

Furthermore, the applied armature voltage adjusts per operational requirements while the source voltage remains steady, affirming the control system's efficient energy regulation to uphold optimal motor performance.

Overall, the graph depicts a responsive and adaptable system with robust energy management capabilities capable of meeting dynamic operational demands.
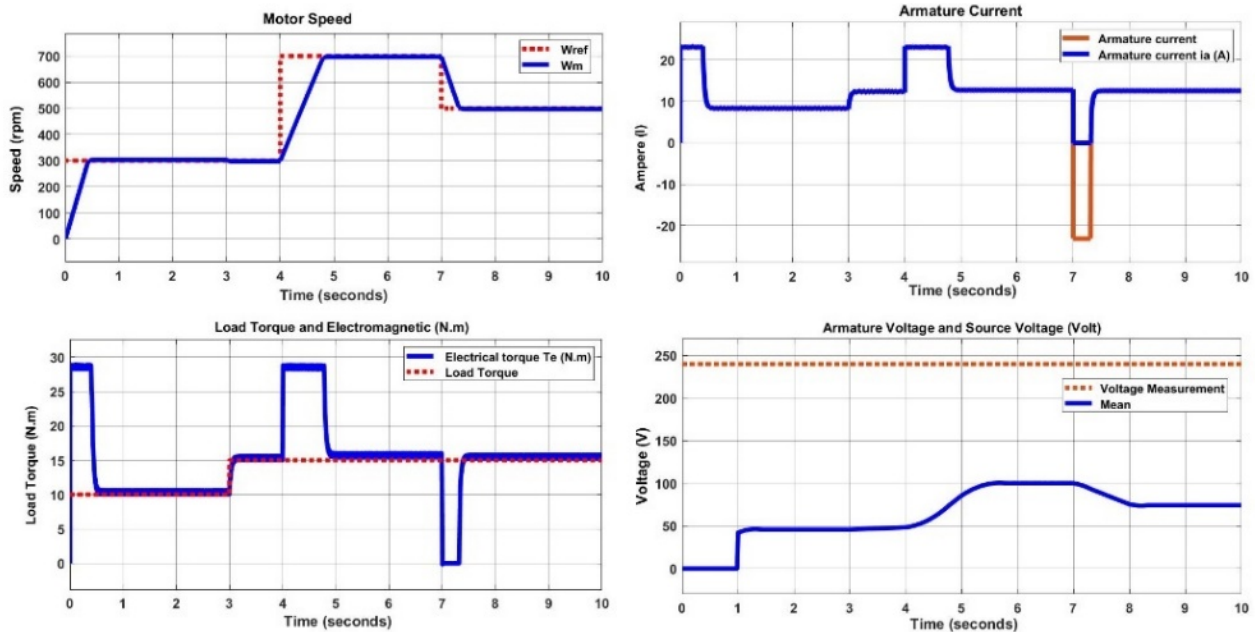

Figure 16. Results of waveforms in the control using ANN

Based on the data illustrated in Figure 16, it can be deduced that employing ANN in the motor control system exhibits consistent and efficient performance, demonstrating a robust capability to adeptly respond to speed and load fluctuations. This adaptability holds significance in industrial contexts where swift and precise adjustments to varying operational conditions are imperative. A comparison between the PI controller and ANN reveals that the utilization of ANN outperforms the PI controller in the control system.

The blue curve represents the reference speed profile, starting at 300 rpm at 0 seconds, increasing to 700 rpm at 4 seconds, and decreasing to 500 rpm at 7 seconds.

Both figures juxtapose the waveforms under PI and ANN control. Under PI control, fluctuations in motor speed surpass the reference speed line, unlike under ANN control, which endeavours to align with the reference line. The assessment of control system trials comparing PID and ANN employs a method of analyzing the response of a second-order system.
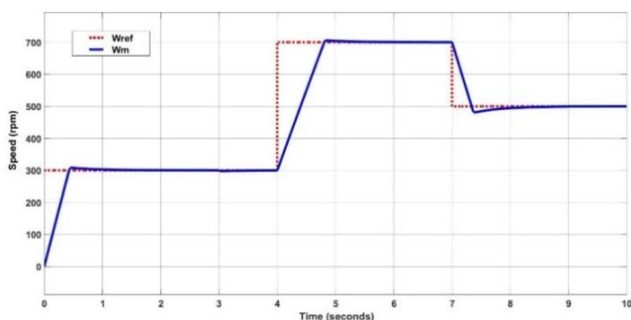
Figure 17. Results on DC motor speed control system using PI

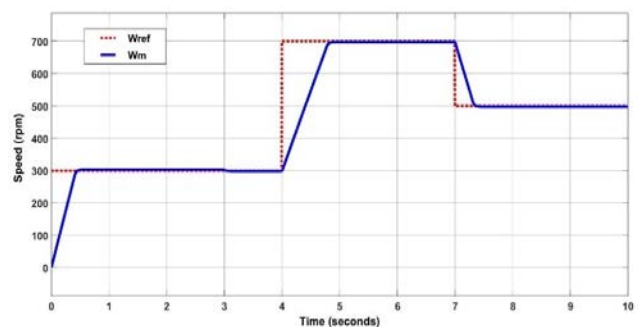*Figure 18. Results on DC motor speed control system using ANN*

Comparative images depicting the control system's performance with PI and ANN can be observed in Figures 17 and 18 below for further elaboration. These diagrams depict motor speed waveforms represented by blue and red colours.

Table 2 delineates the outcomes of the system's response to the DC motor speed test under PI and ANN control.

Table 2. The results of testing system response

Variable Control	Delay Time	Rise Time	Overshoot (%)	Steady State Error
PI	0,214	643,66	2,3 %	7
ANN	0,213	632,11	1,6 %	3

In the system response test results, a comparison between motor speed under PI and ANN control reveals consistent delay times at 0.214. However, a discrepancy arises in the rise time values, with PI control registering 643.66 compared to ANN control's 632.11, indicating an 11.55 difference. The overshoot percentages differ, with PI control at 2.3% and ANN control at 1.67%. The steady-state error yields a value of 7 for both PI and control, while ANN control demonstrates a value of 3.

5. Conclusion

This study involves developing and simulating an intelligent control system employing an ANN algorithm. The investigation compares the speed test outcomes of a single-quadrant DC chopper motor using PI and ANN control techniques. Data from the PI controller are utilized to train the ANN through the back-propagation method. The findings indicate that employing LabVIEW facilitates the real-time processing of precise system response data. ANN control significantly enhances the system response in regulating DC motor speed compared to PI control. Performance metrics such as delay time, overshoot, rise time, and steady-state error demonstrate the superiority of ANN control over PI. However, optimal performance of ANN requires meticulous training, and further research should explore additional factors influencing the efficacy of both control methods.

References:

[1]. Das, S. (2021). Modeling DC Motors and Their Control. *In Modeling for Hybrid and Electric Vehicles Using Simscape*, 47–71.
Doi: 10.1007/978-3-031-01508-3_4

[2]. Samylingam, L., et al. (2024). Green Engineering with Nanofluids: Elevating Energy Efficiency and Sustainability. *Journal of Advanced Research in Micro and Nano Engineering*, 16(1), 19–34.
Doi: 10.37934/armne.16.1.1934

[3]. Annasaheb, K. B., Pathan, K. A., Auti, A. B., & Khan, S. A. (2023). Simulation of Energy Dissipation in BLDC Motor and Analysis of Speed-Acoustic Characteristics. *Journal of Advanced Research in Applied Mechanics*, 111(1), 38–61.
Doi: 10.37934/aram.111.1.3861

[4]. Kolakoti, A., Setiyo, M., Al Husaeni, D. N., & Nandiyanto, A. B. D. (2023). Enhancing heat transfer performance of automotive car radiator using camphor nanoparticles: experimental study with bibliometric analysis. *Teknomekanik*, 6(2), 47–66. Doi: 10.24036/teknomekanik.v6i2.25072

[5]. Moe, K. M., Aung, H. M., Thar, H. A., & Win, Y. Y. (2023). Analysis of energy production design from grid-connected 40 MW large PV power plant. *Teknomekanik*, 6(1), 1–11.
Doi: 10.24036/teknomekanik.v6i1.18972

[6]. Lopez-Gomez, et al. (2020). Influence of PWM Torque Control Frequency in DC Motors by Means of an Optimum Design Method. *IEEE Access*, 8, 80691–80706.
Doi: 10.1109/ACCESS.2020.2990158

[7]. Tyas, R. L., et al. (2023). Risk Assessment of Solid Propellant Rocket Motor using a Combination of HAZOP and FMEA Methods. *Journal of Advanced Research in Fluid Mechanics and Thermal Sciences*, 110(1), 63–78.
Doi: 10.37934/arfmts.110.1.6378

[8]. Alajmi, S., et al. (2022). Simulation of Low Voltage DC-DC Booster Circuit with Improved Switch for Amplification of Biophotovoltaic Cell Output Voltage. *Journal of Advanced Research in Fluid Mechanics and Thermal Sciences*, 90(2), 124–134. Doi: 10.37934/arfmts.90.2.124134

[9]. Daneshjo, N., Pajerská, E. D., Hajduova, Z., Stratyinski, C. D., & Danishjoo, M. (2019). Use of modern software systems for design and realization of prototype of three-dimensional model. *TEM Journal*, 8(2), 346–353.
Doi: 10.18421/TEM82-05

[10]. Reiser, P., Neubert, M., Eberhard, A., Torresi, L., Zhou, C., Shao, C., ... & Friederich, P. (2022). Graph neural networks for materials science and chemistry. *Communications Materials*, 3(1), 93.
Uzair, M., & Jamil, N. (2020, November). Effects of hidden layers on the efficiency of neural networks. In *2020 IEEE 23rd international multitopic conference (INMIC)* (pp. 1-6). IEEE.

[11]. Lim, C. E., Chong, K. H., Sia, C. C. V., Lee, Y. Y., & Lee, M. D. (2024). Numerical Study for Crashworthiness of FSAE Vehicle Chassis via Biomimetic Approach. *Journal of Advanced Research in Applied Sciences and Engineering Technology*, 33(2), 328–339.
Doi: 10.37934/araset.33.2.328339

[12]. Abdolrasol, M. G. M., et al. (2021). Artificial neural networks based optimization techniques: A review. *Electronics (Switzerland)*, 10(21), 1–43.
Doi: 10.3390/electronics10212689

[13]. Buditjahjanto, I. G. P. A., Idhom, M., Munoto, M., & Samani, M. (2022). An Automated Essay Scoring Based on Neural Networks to Predict and Classify Competence of Examinees in Community Academy. *TEM Journal*, 11(4), 1694–1701.
Doi: 10.18421/TEM114-34

[14]. Yüksel, N., Börklü, H. R., Sezer, H. K., & Canyurt, O. E. (2023). Review of artificial intelligence applications in engineering design perspective. *Engineering Applications of Artificial Intelligence*, *118*, 105697.
Doi: 10.1016/j.engappai.2022.105697

[15]. Kadhim, Z. S., Abdullah, H. S., & Ghathwan, K. I. (2022). Artificial Neural Network Hyperparameters Optimization: A Survey. *International Journal of Online and Biomedical Engineering*, *18*(15), 59–87.
Doi: 10.3991/ijoe.v18i15.34399

[16]. Otchere, D. A., Arbi Ganat, T. O., Gholami, R., & Ridha, S. (2021). Application of supervised machine learning paradigms in the prediction of petroleum reservoir properties: Comparative analysis of ANN and SVM models. *Journal of Petroleum Science and Engineering*, *200*, 108182.
Doi: 10.1016/j.petrol.2020.108182

[17]. Folkourng, F., & Sakti, R. H. (2022). The design of expert system to determine the university majoring based on multiple intelligence using forward chaining method. *Journal of Engineering Researcher and Lecturer*, *1*(1), 17–24.
Doi: 10.58712/jerel.v1i1.6

[18]. Koizhanova, A., Magomedov, D., Abdyldayev, N., Yerdenova, M., & Bakrayeva, A. (2023). The effect of biochemical oxidation on the hydrometallurgical production of copper. *Teknomekanik*, *6*(1), 12–20.
Doi: 10.24036/teknomekanik.v6i1.16072

[19]. Guillod, T., Papamanolis, P., & Kolar, J. W. (2020). Artificial neural network (ANN) based fast and accurate inductor modeling and design. *IEEE Open Journal of Power Electronics*, *1*, 284–299.
Doi: 10.1109/OJPEL.2020.3012777

[20]. Heng, S. Y., et al. (2022). Artificial neural network model with different back-propagation algorithms and meteorological data for solar radiation prediction. *Scientific Reports*, *12*(1), 1–
Doi: 10.1038/s41598-022-13532-3

[21]. Mouloodi, S., Rahmanpanah, H., Gohari, S., Burvill, C., & Davies, H. M. S. (2022). Feed-forward back-propagation artificial neural networks for predicting mechanical responses in complex non-linear structures: A study on a long bone. *Journal of the Mechanical Behavior of Biomedical Materials*, *128*, 105079.
Doi: 10.1016/j.jmbbm.2022.105079

[22]. Abdullah, Faye, I., & Aziz, L. A. (2023). Artificial Neural Networks Solutions for Solving Differential Equations: A Focus and Example for Flow of Viscoelastic Fluid with Microrotation. *Journal of Advanced Research in Fluid Mechanics and Thermal Sciences*, *112*(1), 76–83.
Doi: 10.37934/arfmts.112.1.7683

[23]. Masoumi, A., Jabari, F., Ghassem Zadeh, S., & Mohammadi-Ivatloo, B. (2020). Long-Term Load Forecasting Approach Using Dynamic Feed-Forward Back-Propagation Artificial Neural Network. *Studies in Systems, Decision and Control*, *262*, 233–257.
Doi: 10.1007/978-3-030-34050-6_11

[24]. Femi, R., Sree Renga Raja, T., & Shenbagalakshmi, R. (2021). A positive output-super lift Luo converter fed brushless DC motor drive using alternative energy sources. *International Transactions on Electrical Energy Systems*, *31*(2).
Doi: 10.1002/2050-7038.12740

[25]. Shchur, I., & Jancarczyk, D. (2021). Electromagnetic torque ripple in multiple three-phase brushless dc motors for electric vehicles. *Electronics*, *10*(24), 1–25. Doi: 10.3390/electronics10243097

[26]. Feng, N., Yu, H., Zhao, M., Zhang, P., & Hou, D. (2020). Magnetic field-modulated linear permanent- magnet generator for direct-drive wave energy conversion. *IET Electric Power Applications*, *14*(5), 742–750.
Doi: 10.1049/iet-epa.2019.0483

[27]. Hamanah, W. M., Salem, A., & Abido, M. A. (2023). Evaluation of advanced wide bandgap Semiconductor-based DC-DC converter for solar power tower tracker application. *Alexandria Engineering Journal*, *74*, 627–641.
Doi: 10.1016/j.aej.2023.05.042

[28]. Palacín, J., & Martínez, D. (2021). Improving the angular velocity measured with a low-cost magnetic rotary encoder attached to a brushed dc motor by compensating magnet and hall-effect sensor misalignments. *Sensors*, *21*(14), 1–12.
Doi: 10.3390/s21144763

[29]. Bouradi, S., Negadi, K., Araria, R., Boumediene, B., & Koulali, M. (2022). Design and Implementation of a Four-Quadrant DC-DC Converter Based Adaptive Fuzzy Control for Electric Vehicle Application. *Mathematical Modelling of Engineering Problems*, *9*(3), 721–730. Doi: 10.18280/mmep.090319

[30]. Nguyen, N. H., & Nguyen, P. D. (2018). Overshoot and settling time assignment with PID for first-order and second-order systems. *IET Control Theory & Applications*, *12*(17), 2407–2416. Doi: 10.1049/iet-cta.2018.5076